Nuclear Engineering and Technology 51 (2019) 1109–1116

Contents lists available at ScienceDirect

Nuclear Engineering and Technology

journal homepage: www.elsevier.com/locate/net

Original Article

Effects of superimposed cyclic operation on corrosion products activity in reactor cooling system of AP-1000

Fiaz Mahmood, Huasi Hu*, Guichi Lu, Si Ni, Jiaqi Yuan

School of Nuclear Science and Technology, Xi'an Jiaotong University, Xi'an, Shaanxi, 710049, China

ARTICLE INFO

Article history:
Received 18 November 2018
Received in revised form
30 January 2019
Accepted 6 February 2019
Available online 6 February 2019

Keywords:
Corrosion products activity
CPA-AP1000
Cyclic operation
Reactor coolant system
AP-1000

ABSTRACT

It is essential to predict the radioactivity distribution around the reactor cooling system (RCS) during obligatory cyclic operation of AP-1000. A home-developed program CPA-AP1000 is upgraded to predict the response of activated corrosion products (ACPs) in the RCS. The program is written in MATLAB and it uses state of the art MCNP as a subroutine for flux calculations. A pair of cyclic power profiles were superimposed after initial full power operation. The effect of cyclic operation is noticed to be more prominent for in-core surfaces, followed by the primary coolant and out-of-core structures. The results have shown that specific activity trends of ^{56}Mn and ^{24}Na promptly follow the power variations, whereas, ^{59}Fe, ^{58}Co, ^{99}Mo and ^{60}Co exhibit a sluggish power-following response. The investigations pointed out that promptly power-following response of ACPs in the coolant is vital as an instant radioactivity source during leakage incidents. However, the ACPs with delayed power-following response in the out-of-core components are perceived to cause a long-term activity. The present results are found in good agreement with those for a reference PWR. The results are useful for source term monitoring and optimization of work procedures for an innovative reactor design.

1. Introduction

The materials used in a pressurized water reactor (PWR) are posed to a complex environment for a long period of several decades. Despite careful selection, the production of corrosion products (CPs) in the reactor cooling system (RCS) is inevitable. The subsequent activation of CPs by a high neutron flux generates the activated corrosion products (ACPs). The gamma-rays are emitted due to decay of ACPs and they cause major occupational radiation exposure (ORE) [1]. The half-lives of prominent ACPs range from several hours to a few years, as shown in Table 1 [2]. It depicts that radiation caused by the ACPs are particularly important for the designed plant life and even later [3]. The progress has been made in reducing the ORE over the preceding decades, primarily by controlling radioactivity in the RCS. Further development is constrained by understanding the phenomenon of crud formation and transportation for continuously upgrading reactor designs. The crud generation and transportation in the light water reactor (LWRs) is complex, and continuous research is being carried out to grasp it [4].

The current grid connection of new units of AP-1000 in China is an important milestone in the nuclear power history [5]. The enhanced power maneuvering capabilities are mandatory in future PWRs to compete with alternative energy resources [6]. The AP-1000 is a good choice for cyclic operation due to its robust mechanical shim (MSHIM)-based power-maneuvering capabilities. A breadth of advanced operating scenarios can cause unpredictable material damages. More surveillance is required to ensure the reliable operation in such cases. The operating experience depicts that corrosion damages and associated problems are particularly significant in the initial life of the plant [7]. Accurate models are essential to predict the ACPs production and transportation, because blind hotspots can result in accidental ORE. The prediction of the activity behavior in different parts of the primary circuit for cyclic operating scenarios is crucial but challenging.

Several empirical and semi-empirical models have been established to study the CPs transport mechanisms and radioactivity build-up in the light water reactors (LWRs) [8]. Every model has its own standing, but at the same time reserved to deal with a particular set of complex phenomena. The estimation of ACPs behavior in innovative designs, subjected to a variety of operating parameters, still require an extensive research [9]. The assessment

* Corresponding author.
E-mail address: huasi_hu@mail.xjtu.edu.cn (H. Hu).

https://doi.org/10.1016/j.net.2019.02.006

Table 1
Reaction properties of prominent ACPs along with energy of γ-rays.

Sr. #	Reaction	ACPs with half-life	Cross section	Energy of γ-rays (% yield)
1	^{27}Al (n, ∝)^{24}Na (E_n >11.60 MeV) ^{23}Na (n, γ) ^{24}Na (E_n is thermal)	^{24}Na ($T_{1/2}$ = 15.40 h)	6×10^{-4} b 0.53 b	4.10 MeV (100 %)
2	^{58} Fe (n, γ)^{59}Fe (E_n is thermal)	^{59}Fe ($T_{1/2}$ = 45.10 h)	0.90 b	1.17 MeV (99.99%) 1.33 MeV (99.99%)
3	^{98}Mo (n, γ)^{99}Mo (E_n > 3.10 MeV)	^{99}Mo ($T_{1/2}$ = 67 h)	0.45 b	0.78 MeV (8%) 0.74 MeV (8%)
4	^{59}Co (n, γ)^{60}Co	^{60}Co ($T_{1/2}$ = 5.30 y)	20.00 b	1.17 MeV (99.99%) 1.33 MeV (99.99%)
5	^{55}Mn (n, γ)^{56}Mn (E_n is thermal)	^{56}Mn ($T_{1/2}$ = 2.58 h)	13.40 b	2.13 MeV (15%) 1.81 MeV (24%) 0.85 MeV (99%)
6	^{58}Ni (n, p)^{58}Co (E_n is fast)	^{58}Co ($T_{1/2}$ = 70.88 d)	0.146 b	0.81 MeV (99%)

of corrosion behavior of the materials before installation in the reactor-dependent environment is tricky and inadequate. The predictive models of the corrosion mechanisms in different PWR environments are under-developed. The experimental studies are constrained by collection of real samples in harsh PWR conditions. In addition to loop experiments and measurement campaigns, the simulation tools to estimate the RCS contamination has also been felt essential [10].

The solubility of individual CPs at various temperature and pH values is crucial for accurate assessment of corrosion products activity (CPA). To fulfill this purpose, the researchers have recently incorporated a professional water chemistry module in ACPs source term analysis code CATE [11]. In AP-1000, an optimum coolant chemistry is proposed to avoid the corrosion of inner-surface materials in the primary circuit. The lithium in the form of enriched lithium hydroxide is added in the primary coolant to limit the corrosion and the release of CPs within the RCS. The lithium is used in coordination with boron as a pH control agent to guarantee the fuel warranty contract of AP-1000 [12]. The changes in core temperature profile are expected with power variations, which will in turn cause changes in pH values. The concentration of lithium will change with the variation in boron concentration to maintain a specific value of pH [13].

The behavior of ACPs have been investigated by developing computational models for normal operation and also for power and flow transients under linear increase of corrosion [2,14]. The use of different enrichments of boric acid as a chemical shim has shown the significant effect on the primary coolant activity in PWRs [15,16]. The burnable poisons in AP-1000 core and fine power control with grey rods bank provide essential excess reactivity in the beginning of cycle. This is in contrast to chemical shim-based operation, which requires a high boron concentration to provide excess reactivity at the start of cycle. Therefore, MSHIM-based operation in AP-1000 is expected to have peak boron concentration during the cycle instead of beginning of cycle [13]. The MSHIM reactor control is attributed with better chemistry control due to minimum boron variations throughout the cycle. The controls on chemistry provide sufficient protection to the inner-surface materials in the primary circuit by suppressing the corrosion-induced damages [17]. An improved control of pH value during boron-free operation is favorable in reducing the build-up of ACPs and ultimately the radioactive source term. Furthermore, boron-free operation with MSHIM also brings a significant economic benefit by reducing the amount of effluents to be processed.

The investigations on CPA behavior in new reactor design are currently getting more research attention, motivated by the profound operating experience of installed PWRs [1,13,18,19]. The mixed conduction model-based code CAT 1.0 was established to investigate the response of CPs migration process in the RCS of AP-1000 [20,21]. The code is also capable of calculating the corrosion-inhabitation impact caused by Zn injection, but it does not handle the activation of CPs. The computer program Corrosion Products Activity in AP-1000 (CPA-AP1000) was established to investigate the response of CPA in RCS for normal operating conditions as well as design-based maneuverings of power [22–24]. The aim of the present work is to investigate the radioactivity hazard associated with the ACPs produced during cyclic operation. The assumptions of the mathematical model of CPA-AP1000 are used and the code is updated to incorporate the cyclicoperating scenarios.

2. Model formulation

The model is developed by considering exchange processes in various parts (primary coolant, in-core, and out-of-core structural materials) of the RCS. The detail of transfer mechanisms is labeled in Fig. 1. The formulation of the time-dependent response of ACPs in the RCS is based on subsequent postulates [23,24]. The composition of CPs is directly related to the chemical composition of material being originally corroded. The corrosion of the RCS materials is uniform and homogeneous. The intrinsic activity is considered ignorable and the deposition of impurities on the wetted surfaces is

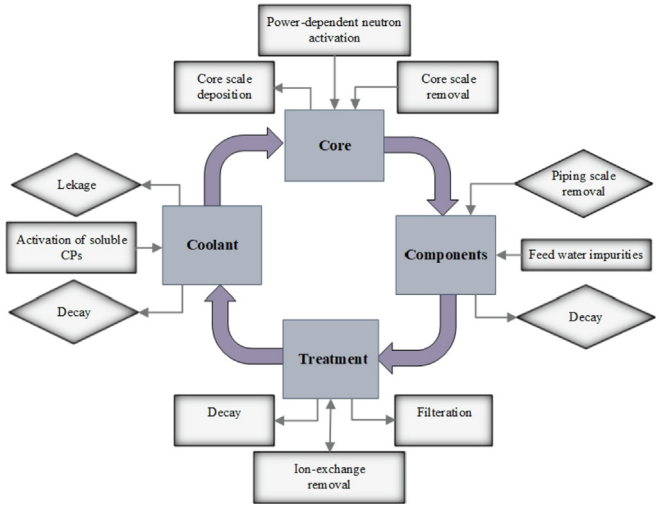

Fig. 1. Transfer mechanisms for modeling ACPs in the RCS during normal and cyclic operation.

relative to their concentration in the coolant. The removal of impurities from the coolant by ion exchangers (IXs) and filters is relative to their amount present in the primary water. The model treats neutron flux as a characteristic of the reactor thermal power. The variation in power-levels is regarded in terms of operational power $p(t)$, power parameter $c(t)$ for normal and cyclic operation, and rated power p_r as following

$$p(t) = c(t)p_r \tag{1}$$

The power parameter $c(t)$ expresses linear changes in the power levels by the following relation

$$c(t) = \begin{cases} p_s & , t < t_i \\ p_s - \mu(t - t_i) & , t_i \le t < t_f \\ p_e & , t \ge t_f \end{cases} \tag{2}$$

where p_s and p_e denote operating-power, in terms of percentage rated power, before beginning and after the termination of cyclic operation, at time t_i and t_f respectively. The slope of any linear variation in the power during normal or cyclic operation is represented by μ.

The activation process of CPs is subjected to the time T_L(s) required for the circulation of a particle in the primary circuit, which can be estimated as LT_c/H, where L(cm) denotes the loop length of the circuit and T_c(s) is the core residence time. The parameter T_c is linked with core height H(cm), coolant densityρ (g/cm^3), area of flow path A (cm^2) and mass flow rate w(g/s) as per relation $H\rho A/w$. The neutron flux density ϕ_ε(neutrons/cm^2·s) is by the following expression

$$\phi_\varepsilon = \frac{1 - e^{-\lambda T_c}}{1 - e^{-\lambda T_L}}\phi_0 \tag{3}$$

where ϕ_0 is the effective group flux (neutrons/cm^2·s) and λ(s^{-1}) is the decay constant of the radioisotope.

The quantities N_w, N_p and N_c symbolize concentration (atoms/cm^3) of target nuclides in the water, and surfaces of piping and core structures respectively. Similarly, n_w, n_p, and n_c denote the concentration (atoms/cm^3) of ACPs in the water, and on the inner surfaces of out-of-core and in-core structures respectively. The transformation rate of ACPs in the primary water is described as

$$\frac{dn_w}{dt} = \sigma c(t)\phi_\varepsilon N_w - \left(\sum_j \frac{\varepsilon_j Q_j}{V_w} + \sum_k \frac{l_k}{V_w} + \lambda\right) n_w + \frac{k_p}{V_w} n_p + \frac{k_c}{V_w} n_c \tag{4}$$

where σ denotes the cross section for the generation of the radioactive substances from the target species. Different removal rates are described by $\varepsilon_j Q_j$ of as following

$$\varepsilon_j Q_j = \varepsilon_c Q_c + \varepsilon_p Q_p + \varepsilon_i Q_i + \varepsilon_f Q_f \tag{5}$$

where the quantities $\varepsilon_c Q_c$, $\varepsilon_p Q_p$, $\varepsilon_i Q_i$, $\varepsilon_f Q_f$ represent removal rates (cm^3/s) by core, pipe, IX and filter correspondingly. The measured values of exchange-rates for a typical PWR are described in Table 2 [2]. The rate (cm^3/s) of water lost during the kth leak is accounted for by the term l_k. The removal rate (cm^3/s) from the scale on core and piping surfaces is denoted by k_c and k_p correspondingly. The generation of ACPs is represented by the first-term of equation (4), the second-term refers to the removal of ACPs due to decay, IX purification, and deposition on filter, core and piping. The rates for re-incorporation of activity into the primary water on account of ACPs erosion from piping and core surfaces are defined by the third and the fourth-terms of equation (4).

Table 2
The measured values of exchange-rates for a typical PWR.

Rate description	Value and unit
Core deposition	$\varepsilon_c Q_c/V_c = 8.81 \times 10^{-6} s^{-1}$
Piping deposition	$\varepsilon_p Q_p/V_w = 1.00 \times 10^{-6} s^{-1}$
IX removal	$\varepsilon_I Q_I/V_w = 5.70 \times 10^{-5} s^{-1}$
Core resolution	$K_c/V_c = 4.41 \times 10^{-6} s^{-1}$
Piping resolution	$K_p/V_p = 5.04 \times 10^{-6} s^{-1}$
Primary coolant volume	$V_w = 1.37 \times 10^7 cm^3$
Core scale volume	$V_c = 9.08 \times 10^6 cm^3$
Piping scale volume	$V_p = 1.37 \times 10^6 cm^3$
Corrosion area	$S = 1.01 \times 10^8 cm^2$
Avg. Corrosion rate	$C_0 = 2.40 \times 10^{-13}\ g/cm^2 \cdot s$

The concentration of target-nuclide in primary water transforms at the rate given by

$$\frac{dN_w}{dt} = -\left(\sum_j \frac{\varepsilon_j Q_j}{V_w} + \sum_k \frac{l_k}{V_w} + \sigma c(t)\phi_\varepsilon\right) N_w + \frac{k_p}{V_w} N_p + \frac{k_c}{V_w} N_c + S_w \tag{6}$$

$$S_w = \frac{C_0 S N_0 f_n f_s}{V_w A} \tag{7}$$

where C_0 symbolizes corrosion rate (g/cm^2·s), S denotes area (cm^2) of the system interacting with water, N_0 represents Avogadro's Number (6.02 × 10^{23} atoms/g·mole), Adescribes atomic mass of target-nuclide (g/mol), f_n and f_s stand for the natural and structural abundance of target-nuclide in the RCS materials.

The transformation rate of ACPs on the surface of core is described by

$$\frac{dn_c}{dt} = \sigma c(t)\phi_0 N_c + \frac{\varepsilon_c Q_c}{V_c} n_w - \left(\frac{k_c}{V_c} + \lambda\right) n_c \tag{8}$$

The rate at which target-nuclei vary in the core scale is given by

$$\frac{dN_c}{dt} = \frac{\varepsilon_c Q_c}{V_c} N_w - \left(\frac{k_c}{V_c} + \sigma c(t)\phi_0\right) N_c \tag{9}$$

where V_c denotes the volume (cm^3) of scale deposited on the core surfaces.

The rate of active material transformation on the surface of out-of-core piping structure is described by the following equation

$$\frac{dn_p}{dt} = \frac{\varepsilon_p Q_p}{V_p} n_w - \left(\frac{k_p}{V_p} + \lambda\right) n_p \tag{10}$$

where V_p symbolizes the volume (cm^3) of scale deposited on the surface of piping structure.

The target-nuclei on the scale of piping transform at the rate given by the following equation

$$\frac{dN_p}{dt} = \frac{\varepsilon_p Q_p}{V_p} N_w - \frac{k_p}{V_p} N_p \tag{11}$$

The above-mentioned set of ordinary differential equations (ODEs) is suitable for the estimation of ACPs behavior during normal and cyclic operating scenarios. The derived equations are appropriate in any case of corrosion pattern. In this research, we have assumed a uniform corrosion and ignored the effects of space-distribution.

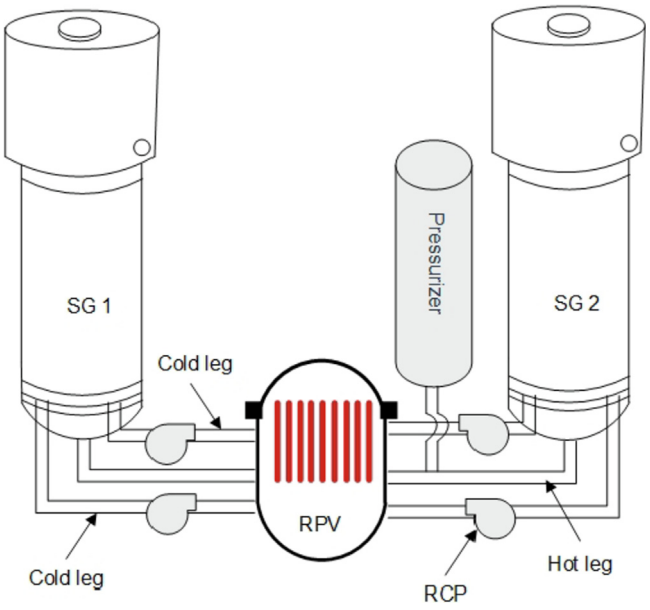

Fig. 2. The configuration of key components of RCS.

3. RCS configuration and flux calculations

The main objective of RCS is heat transmission from the core to steam generators (SGs) and confine the radioactivity within the circuit. The system pressure boundary has a high degree of integrity to provide a barrier against the radioactivity release. The AP-1000 owns a two-loop RCS, having one SG and a pair of reactor coolant pumps (RCPs) in each loop [12]. The purpose of RCPs is circulation of the water through the reactor pressure vessel (RPV) and the SGs for heat transfer purposes. The pressurizer maintains pressure in the RCS with the actuation of heaters and water spray. The wetted surfaces in the RCS in contact with water cause the generation of CPs and subsequently the ACPs are formed. The surfaces in contact with coolant are either made-up of or lined with corrosion-tolerant materials. The structural material choices are limited to SS, Ni-Cr-Fe alloys, Co-based alloys, and I690 TT for SG tubes. A layout of the RCS with key components is shown in Fig. 2.

The AP-1000 core is designed for 3400 MW_{th} power, 18-months cycle length and discharge burnup of 60,000 MWd/tU. The core is enclosed with thick SS reflectors (38 cm) from radial direction, whereas a thick layer (25 cm) of light water covers it from both top and bottom [23]. The reactor core comprises fuel assemblies (157) combined with control and structural components. The fuel enrichment in the fuel assemblies of first-core varies from 2.35 w/o to 4.50 w/o. Each fuel assembly (17 × 17) comprises fuel rods (264), control rod guide tubes (24), and a central thimble. The distribution scheme of enriched assemblies in core and configuration of fuel assembly of AP-1000 are depicted in Fig. 3.

The Discrete Burnable Absorbers (PYREX) and Integrated Fuel Burnable Absorber (IFBA) rods are structured in three and five diverse patterns to construct total nine different types of the fuel assembly. The PYREX and IFBA rods mean to regulate the excess reactivity and would be removed from the core at the end of the first-cycle. The design values of the key parameters of AP-1000 are given in Table 3 [12,24].

3.1. The computational hierarchy for CPA-AP1000

The computational scheme developed for the computer code, CPA-AP1000, is improved for cyclic operating modes. The program comprises two loops; one computes the response of ACPs for normal or cyclic operating scenarios, whereas other transfers over various ACPs. As a first step, the group fluxes are calculated via Tally-F4 of MCNP. It is important to notice that the quantities of flux given by the Tally-F4 are normalized to a single neutron source. The results should be appropriately scaled to acquire the absolute assessment. Therefore, scaling factor corresponding to the anticipated power is applied to Tally-F4 group fluxes, using following relation [22,24].

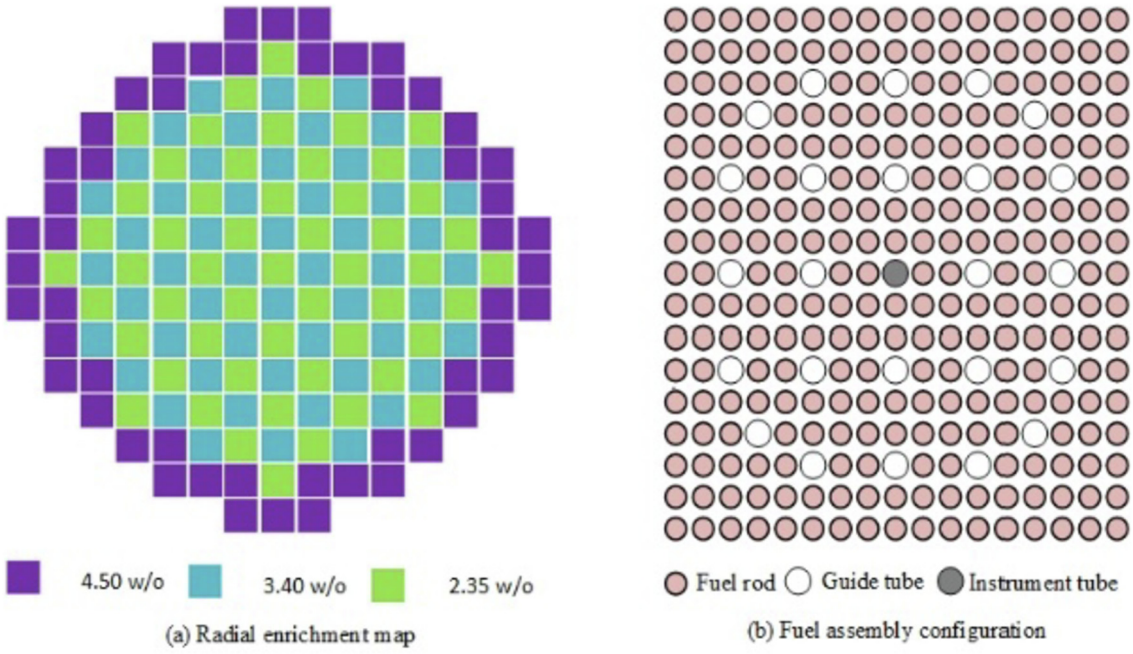

Fig. 3. The distribution (a) scheme of enriched assemblies in the core and (b) configuration of fuel assembly.

Table 3
The design values of key parameters for AP-1000.

Parameter	Design value	Parameter	Design value
Power		Type	Vertical U-tube
Thermal power (MW)	3400	Material	I690 TT
Electrical power (MW)	1090	Fuel	
Power density (MW/m$^{3)}$	109.70	No. of FA	157
Specific power (kW/kg U)	40.20	Dimension of rod array	17 × 17
Core		Rods/assembly	264
Diameter (m)	3.04	Pitch of rod (mm)	12.60
Height (m)	4.27	Clad thickness (mm)	0.5715
Loops		Fuel loading, UO_2 (kg)	95974
Cold legs	4	Material	UO_2
Hot legs	2	Pellet diameter (mm)	8.1915
ID of Hot leg (cm)	78.74	Number of fuel rods	41448
ID of Cold leg (cm)	55.88	Rod, OD (mm)	9.50
RCP		Diameter gap (mm)	0.1651
Number of RCPs	4	FA dimension (mm × mm)	214 × 214
Type	Sealless	Clad material	ZIRLO
Pump power (MWt)	15	Fuel pellet length (mm)	9.83
Pressurizer		Enrichment levels	2.35w/o to 4.50w/o
Number of units	1	Mass of UO_2/m (kg/m)	6.54
Height (cm)	1277.62	Coolant	
Inside diameter (cm)	254	Pressure (MPa)	15.51
SG		Inlet temp. (°C)	279.44
No. of units	2	Avg. temp. in core (°C)	303.39
SG power (MWt/unit)	1707.5	Flow rate of RPV (kg/s)	14300.76

$$\phi_0 = \frac{P\,(Watt)\cdot \overline{\nu}\,(n/fission)}{1.6023.10^{-13}(\mathrm{J}/MeV)\; w_f\;(MeV/fission)}\;\phi_{F4} \tag{12}$$

where P denotes reactor power, $\overline{\nu}$ symbolizes for avg. neutrons/fission, w_f represents the energy emitted/fission and ϕ_{F4} designates the neutron flux from Tally-F4 of MCNP. After scaling of the group fluxes, program tests for reactor operation mode; i.e. either normal or cyclic operation. Subsequently group fluxes are selected as per operating scenario. The RK-4 method is employed for solution of the set of equations developed in Section 2. The program iterates over given reactor operation time and selected ACPs. The overall computational scheme of updated CPA-AP1000 is shown in Fig. 4.

4. Results and discussions

The measured values of deposition and re-solution exchange-rates for piping and core surfaces, and other specific properties used in the investigations are as mentioned in Table 2. The simulations were initiated at time t = 0, allowing the initial normal operation of the reactor without impurities. The removal-rate by IX is the most sensitive parameter, so an optimum value (600 cm^3/s) was calculated employing the approach developed in our previous research [23].

According to the recent version of the European Utilities Requirements (EUR), a modern NPP should as a minimum be capable of daily load cycling operation between 50% and 100% of its rated power [25]. Under cyclic operation, the reactor is anticipated to experience a transient from full power to minimum load and back to full power for several times in a week. A pair of same demand profile with typical minimum load of 50% was selected to investigate the impact of consecutive cyclic operation on the ACPs. The repeated power transients were meant to assess the behavior of ACPs in case of superimposition of cyclic operating scenarios. Two identical operation profiles, each sustaining for time duration 4-3-6-3-8 as per power demand 100-50-100-100 considered for this study are shown in Fig. 5.

The operation profile depicts that reactor operates at 100% p_r for 4 h, followed by a 3 h power decline to approach operating power to 50% p_r. Then power is maintained at 50% p_r for 6 h, subsequently power rises for 3 h to approach 100% p_r, and it is maintained at 100% p_r for next 8 h. The same operating profile is consecutively repeated.

4.1. ACPs behavior in the primary coolant

The response of ACPs in the RCS was simulated using CPA-AP1000. The reactor was operated at 100% p_r up to 750 h and demand profiles as described above were applied during the reactor operation (750 h - 798 h). The consecutive power transients were meant to assess the behavior of ACPs in case of superimposed cyclic operating scenarios. The response curves of ACPs have demonstrated rapid evolution at the start due to substantial corrosion during preliminary reactor operation. Afterward, ACPs begin accumulating on the system walls and also removed by the IX and filters. The balance of removal and deposition of the ACPs lead to an equilibrium state after a particular operating period. The ACPs behavior in the primary coolant for reactor operation in normal and sequential cyclic operating scenarios is shown in Fig. 6.

The first cyclic-profile was incorporated at 750 h. The power remains constant up to 754 h and so does the saturation value of the ACPs. However, with decrease in power from 100% p_r to 50% p_r in 3 h during 754 h–757 h, the specific activity of the corresponding ACPs also reduces. The specific activity of ^{56}Mn and ^{24}Na is noticed to rapidly decrease with reduction in the power. However, the specific activity of other ACPs ^{59}Fe, ^{58}Co, ^{99}Mo and ^{60}Co decreases slowly during this power-decreasing period (754 h - 757 h). For the duration (757 h - 763 h) of constant power at 50% p_r, the specific activity of corresponding ACPs remains decreasing. For the reactor power increase (763 h - 766 h) in the following 3 h from 50% p_r to 100% p_r, the specific activity of corresponding ACPs starts increasing. For the following period (766 h - 774 h) of constant full power, the specific activity of corresponding ACPs keeps on increasing. Subsequently, another identical cyclic-profile was incorporated for the reactor operation during 774 h–798 h. The specific activity of ACPs during power variation follows similar trend of increase and decrease as previously. However, the initiation of power-following response for second cyclic-profile is not from the full-power, in contrast to for first cyclic-profile. The

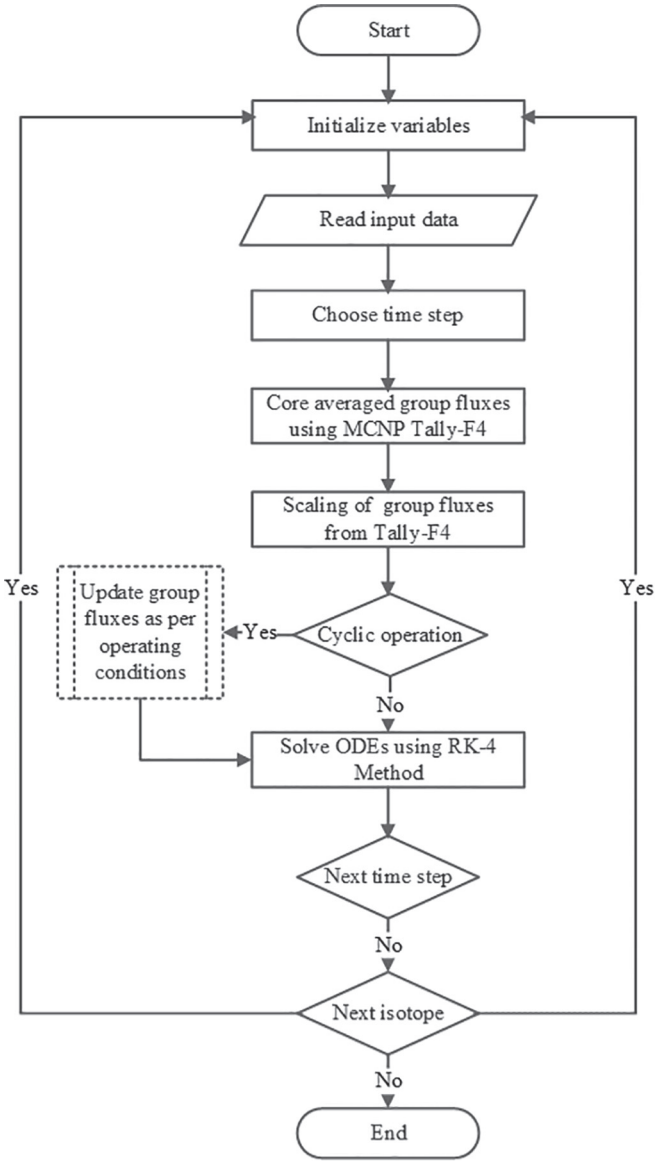

Fig. 4. The computational hierarchy of CPA-AP100 for normal and cyclic operating scenarios.

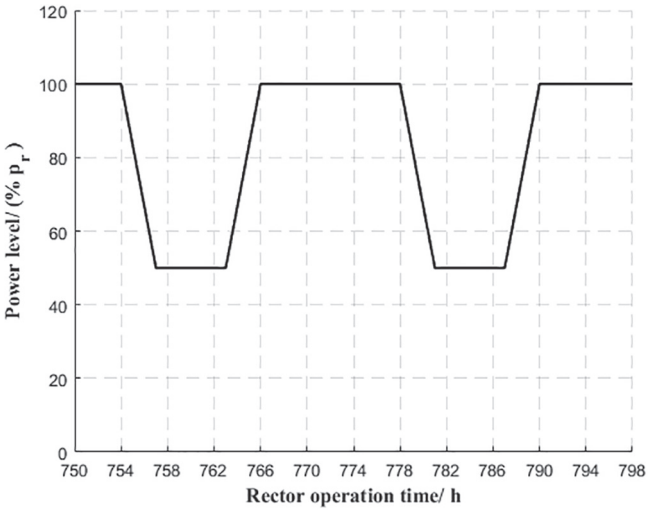

Fig. 5. The identical power demand profiles for superimposed cyclic operating scenarios.

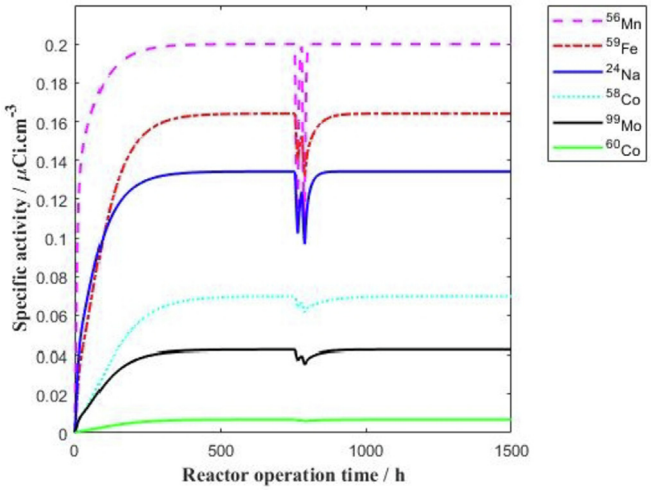

Fig. 6. ACPs behavior of in primary water for normal and cyclic operation.

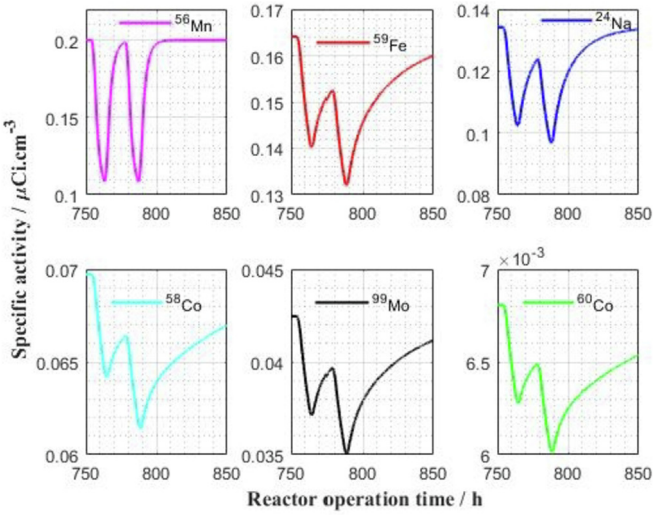

Fig. 7. ACPs response in primary water during superimposed cyclic operation.

detailed behavior of ACPs in primary coolant during superimposed cyclic operation scenarios is shown in Fig. 7.

After the termination of the cyclic operation, the rector successively followed full power for the rest of period (798 h - 1500 h). It is seen that the corresponding ACPs attain saturation state after a certain period of operation at 100% p_r. The pre-transient and post-transient full-power response curves and saturation values of ACPs are compared with the corresponding values of a typical PWR and found in reasonable agreement [23]. It shows that CPA-AP1000 can reliably predict the behavior of ACPs during cyclic operation. The detailed behavior of ACPs on inner walls of the structural materials inside and outside the core, under cyclic operating scenarios is discussed in the following sections.

4.2. ACPs behavior on the out-of-core surfaces under cyclic operation

The specific activity of ACPs on the inner walls of out-of-core piping is the lowest among all circuit components, as depicted by

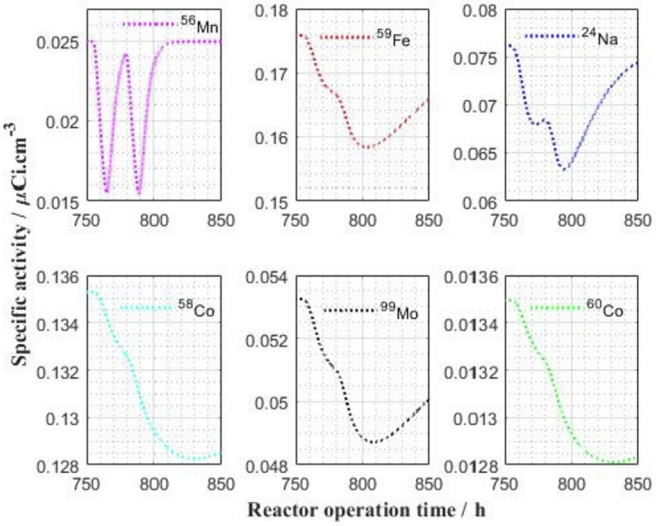

Fig. 8. ACPs response on the inner surfaces of out-of-core piping under superimposed cyclic operation.

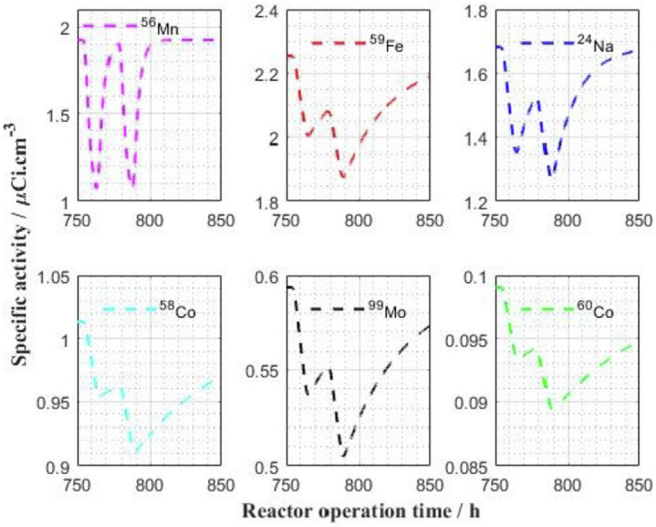

Fig. 9. ACPs response on the surfaces of in-core structures under superimposed cyclic operation.

Fig. 8. It is mainly because the ACPs on the piping structures are not directly subjected to the neutron flux. The scale on in-core surfaces is eroded, subsequently dissolved in the coolant and transported to the out-of-core components. Therefore, the activity on out-of-core surfaces is subjected to the exposure of CPs by the neutron flux inside the reactor core and migration of resultant ACPs in the coolant.

The results demonstrate that power-following response of ACPs on the inner surfaces of out-of-core piping is comparatively lethargic. It depicts that though power varies the specific activity due to ACPs does not promptly change. The activity from ^{59}Fe, ^{58}Co, ^{99}Mo and ^{60}Co demonstrate particularly lethargic power-following response. The lethargic power-following response of ACPs on the out-of-core surfaces own important dosimetry impact, because frequent access is required for these components. However, the response of ^{56}Mn and ^{24}Na is power-following as compared with other ACPs on the out-of-core surfaces. It is vital as these ACPs will cause an instant source of activity following the power variation.

4.3. ACPs behavior on the in-core surfaces under cyclic operation

The response of ACPs on the in-core surfaces follows the variation in operating power levels at different rates. The results have shown that the ACPs (^{56}Mn, ^{24}Na) with short half-lives promptly follow the operating power levels as compared to the ACPs (^{59}Fe, ^{58}Co, ^{99}Mo and ^{60}Co) with long half-lives. The trend of specific activity of ACPs is decreasing with reduction in power. If power is increased, the activity starts building up. However, the results for period of constant power operations depicts that ACPs behavior is also subjected to pre and post powers in addition to existing constant power. The trends of activity due to all of the ACPs in this case, are similar to as that for the coolant. However, the corresponding ACPs on the in-core structures is noticed to be the highest among all components of RCS. It is mainly due to fact that the in-core structures are directly and extensively exposed to the neutron flux. The activity of corresponding ACPs on the in-core surfaces for superimposed cyclic operation scenarios is shown in Fig. 9.

In the course of cyclic operation, the structures inside the reactor core have depicted major sources of activity, because of sustained and long-term neutron exposure inside the core. The primary coolant is the second highest source of activity but it is more important being a mobile source of activity in the RCS. The specific activity of the corresponding ACPs on the out-of-core surfaces has shown the lowest activity contribution and the slowest power-following impact. It is interesting to note that although reactor operates at a constant power level during a particular period, the specific activity may or may not be constant. If operation at a constant power-level is preceded by an increasing or decreasing power transient, the specific activity of ACPs still carry the effect of previous operating conditions. It is due to fact that the specific activity caused by the corresponding ACPs does not immediately saturate. A time lag is expected in such cases because the approach to saturation is subjected to various time-dependent build up and decay mechanisms.

5. Conclusions

Two identical and superimposed cyclic operation profiles were incorporated to the reactor initially operating in normal operation mode. The cyclic operation based response of ^{56}Mn, ^{24}Na, ^{59}Fe, ^{58}Co, ^{99}Mo and ^{60}Co in the primary water, and on the surfaces of in-core and out-of-core structural materials has been focused in this research. The ^{56}Mn and ^{24}Na have shown a prompt power-following activity variation, which is a noticeable instant radioactivity source. This is critical regarding immediate access to RCS components during the loss of coolant accidents (LOCAs). The activity due to ^{59}Fe, ^{58}Co, ^{99}Mo and ^{60}Co has been noticed least adaptable to follow the power instabilities during cyclic operation. This implies that these long-lived ACPs will sustain as a substantial source of activity for longer periods despite power variations. The pre-transient and post-transient results for ACPs in AP-1000 are identical and in reasonable agreement with the results of a reference PWR.

The results have demonstrated that the highest specific activity corresponds to ACPs associated with in-core surfaces, and subsequently by the primary water and out-of-core piping surfaces during entire superimposed cyclic operation. The study has revealed an assessment of the ACPs behavior for anticipated cyclic operating scenarios in AP-1000. It is useful to perceive the dose levels adjacent to the primary circuit components, and successfully implement the ALARA principle to optimize the work procedures. The results are also helpful for source term monitoring and

improvement in the radiation shielding design. Further studies are required to predict the CPA response for a variety of anticipated transient conditions.

Acknowledgment

This research was supported by the China Scholarship Council (2016GXZO22) and Major Project of National Science & Technology (MTR-ZB01K01W16-004). We also gratefully acknowledge the funding supports by Shanghai Nuclear Engineering Research & Design Institute and Nuclear Power Institute of China.

References

[1] J. Zhang, L. Li, S. He, W. Song, Y. Fu, B. Zhang, Y. Chen, Development of a three-zone transport model for activated corrosion products analysis of Tokamak Cooling Water System, Fusion Eng. Des. 109–111 (2016) 407–410.
[2] M. Rafique, N.M. Mirza, S.M. Mirza, Kinetic study of corrosion product activity in primary coolant pipes of a typical PWR under flow rate transients and linearly increasing corrosion rates, J. Nucl. Mater. 346 (2005) 282–292.
[3] J.S. Song, H.J. Cho, M.Y. Jung, S.H. Lee, A study on the application of CRUDTRAN code in primary systems of domestic pressurized heavy-water reactors for prediction of radiation source term, Nuclear Eng. Technol. 49 (2017) 638–644.
[4] M.P. Short, The particulate nature of the crud source term in light water reactors, J. Nuc. mat. 509 (2018) 478–481.
[5] World Nuclear News, Fourth Chinese AP1000 Connected to Grid [cited 2018 17-11-2018], 2018. Available from, http://world-nuclear-news.org/Articles/Fourth-Chinese-AP1000-connected-to-grid.
[6] R. Loisel, V. Alexeeva, A. Zucker, D. Shropshire, Load-following with nuclear power: market effects and welfare implications, Prog. Nucl. Energy 109 (2018) 280–292.
[7] E. Chajduk, A. Bojanowska-Czajka, Corrosion mitigation in coolant systems in nuclear power plants, Prog. Nucl. Energy 88 (2016) 1–9.
[8] M. Rafique, N. Mirza, S. Mirza, M.J. Iqbal, Review of computer codes for modeling corrosion product transport and activity build-up in light water reactors, Nukleonika 55 (2010) 263–269.
[9] IAEA, Modelling of Transport of Radioactive Substances in the Primary Circuit of Water-Cooled Reactors, IAEA-TECDOC-1672, Viana, Austria, 2012.
[10] M. Benfarah, M. Zouiter, T. Jobert, F. Dacquait, M. Bultot, J.-B. Genin, PWR circuit contamination assessment tool. Use of OSCAR code for engineering studies at EDF, EPJ Nucl. Sci. Technol. 2 (2016) 1–5.
[11] Y. Fu, J. Zhang, L. Li, Y. Chen, Solubility calculation of the corrosion products in water-cooled reactors and its application in CATE code, Fusion Eng. Des. 125 (2017) 664–668.
[12] Westinghouse, AP1000 design control document, Rev. 19 (2011). https://www.nrc.gov/docs/ML1117/ML11171A500.html.
[13] Q. Guo, J. Zhang, S. Fang, Y. Chen, Calculation and analysis of water activation products source term in AP1000, Prog. Nucl. Energy 109 (2018) 66–73.
[14] F. Deeba, A.M. Mirza, N.M. Mirza, Modeling and simulation of corrosion product activity in pressurized water reactors under power perturbations, Ann. Nucl. Energy 26 (1999) 561–578.
[15] J.I. Malik, N.M. Mirza, S.M. Mirza, Time-dependent corrosion product activity in a typical PWR due to changes in coolant chemistry for long-term fuel cycles, Prog. Nucl. Energy 58 (2012) 100–107.
[16] R. Nasir, S.M. Mirza, N.M. Mirza, Evaluation of corrosion product activity in a typical PWR with extended cycles and flow rate perturbations, World J. Nucl. Sci. Technol. 07 (2017) 24–34.
[17] O.N.R. Reactor, Chemistry Assessment of the Westinghouse AP1000 Reactor, Office for Nuclear Regulation, 2011. http://www.onr.org.uk/new-reactors.
[18] A.S. Zhilkin, E.P. Popov, Modeling transport of radioactive products of corrosion in loops with sodium coolant, At. Energ. 119 (2015) 37–45.
[19] J.B. Génin, L. Brissonneau, T. Gilardi, OSCAR-Na, A new code for simulating corrosion product contamination in SFR, Metall. Mat. Trans. E. 3E (2016) 291–298.
[20] J. Jia, Research on Modeling the Corrosion, Activity and Transport Proceeds in PWR Primary Circuits [Academic], Xi'an Jiaotong University, Xi'an, China, 2016.
[21] S. Mo, J. Jia, B. Yichen, S. Xiuqiang, D. Wang, X. Xu, Y. Xie, H. Hu, Modelling of materials corrosion inside RCS based on mixed-conduction model, September, in: Proceedings of 8th International Symposium on Symbiotic Nuclear Power Systems for 21st Century, 2016, pp. 26–28. Chengdu, China.
[22] F. Mahmood, H. Hu, L. Cao, Buildup and decay analysis of corrosion products activity in primary coolant loop of AP-1000, in: 26th International Conference on Nuclear Engineering London, England, 2018, pp. 22–26. July.
[23] F. Mahmood, H. Hu, L. Cao, Dynamic response analysis of corrosion products activity under steady state operation and Mechanical Shim based power-maneuvering transients in AP-1000, Ann. Nucl. Energy 115 (2018) 16–26.
[24] F. Mahmood, H. Hu, L. Cao, G. Lu, S. Ni, J. Yuan, Evaluation of activated corrosion products in primary coolant circuit of AP-1000 under grid frequency stability mode, Ann. Nucl. Energy 125 (2019) 138–147.
[25] EUR, Europian utility Requirements for LWR nuclear power plants, vol. 2, Revisiones Cáncer (2001). http://www.europeanutilityrequirements.org.